Available online at www.sciencedirect.com
ScienceDirect
Journal of Volcanology and Geothermal Research 156 (2006) 252–265
Journal of volcanology and geothermal research
www.elsevier.com/locate/jvolgeores

Petrogenesis of dacite in an oceanic subduction environment: Raoul Island, Kermadec arc

Ian E.M. Smith [a,*], Timothy J. Worthington [a,1], Richard C. Price [b], Robert B. Stewart [c], R. Maas [d]

[a] *Department of Geology, University of Auckland, PB92019, Auckland, New Zealand*
[b] *School of Science and Engineering, University of Waikato, P B 3105 Hamilton, New Zealand*
[c] *Soil and Earth Sciences, INR, Massey University, PB 11-222, Palmerston North, New Zealand*
[d] *Department of Earth Sciences, La Trobe University, Bundoora, Vic. 3083, Australia*

Received 24 February 2005; accepted 2 March 2006
Available online 27 April 2006

Abstract

Raoul Volcano in the northern Kermadec arc is typical of volcanoes in oceanic subduction systems in that it is composed mainly of low-K high-Al basalts and basaltic andesite. However, during the last 4 ka Raoul Volcano has produced mainly dacite magma in pyroclastic eruptions associated with caldera formation. The rocks produced in these episodes are almost aphyric containing only sparse crystals of plagioclase, clinopyroxene, orthopyroxene and magnetite. These apparent phenocrysts have chemical compositions that suggest that they did not crystallise from melts with the chemical composition of their host rocks. Rather they are xenocrysts and only their rims show evidence for crystallisation from their host melt. Chemical compositions of samples of the dacites show that each eruption has tapped a distinct magma batch. Compositional variations through the analysed suite cannot be accommodated in any reasonable model of fractional crystallisation from likely parental magma compositions. The hypothesis that best fits the petrology of Raoul Island dacites is one of crustal anatexis. This model requires heating of the lower crust by a magma flux to the point where dehydration melting associated with amphibole breakdown produces magma from a preconditioned source. It is suggested that Raoul is passing through an adolescent stage of development in which siliceous melts are part of an open system in which felsic and mafic magmas coexist.

Keywords: oceanic subduction; Kermadec arc; crustal anatexis; fractional crystallisation; dacite

1. Introduction

Despite the fact that nearly 40% of global subduction takes place somewhere other than at continental margins (Leat and Larter, 2003) intra-oceanic subduction systems are disproportionately less well studied than their continental counterparts. This is primarily because they are mostly submerged below sea level. Oceanic arc systems are thought to represent a first stage in the development of continental crust from oceanic materials and are generally considered to be dominated by relatively mafic magma compositions (basalt–basaltic andesite). Oceanic subduction systems are simpler than their continental counterparts because their underlying

* Corresponding author. Tel.: +64 9 3737435x87416; fax: +64 9 3737435.
E-mail address: ie.smith@auckland.ac.nz (I.E.M. Smith).
[1] Present address: University of Kiel, Olshausenstrasse 40, 24118 Kiel, Germany.

0377-0273/$ - see front matter © 2006 Elsevier B.V. All rights reserved.
doi:10.1016/j.jvolgeores.2006.03.003

crust does not contain older sialic components and they commonly have a shorter history of subduction.

Intra-oceanic arcs are built upon modified oceanic crust and located far from continental land masses. Lavas with >63 wt.% SiO_2 are rare in these arcs (e.g. Bonin–Mariana (Bloomer et al., 1989) South Sandwich (Pearce et al., 1995). Nevertheless, recent caldera forming eruptions of dacite do feature in arc segments characterised by tectonic complexity and crustal extension; for example, the central Vanuatu (Crawford et al., 1988; Robin et al., 1993; Monzier et al., 1994), the west Aleutian arc (Miller, 1995), and the Izu–Bonin arc (Gill et al., 1992; Fiske et al., 2001; Tamura and Tatsumi, 2002). Dacite genesis in this environment is usually ascribed to fractional crystallisation of a mafic parent (cf Ewart et al., 1973; Gill et al., 1992) although models involving dehydration melting have also been proposed (e.g. Beard, 1995; Tamura and Tatsumi, 2002).

It is increasingly evident that silicic magmas are an important component of intraoceanic arcs, often forming mafic–felsic bimodal series associated with calderas (e.g. Tamura and Tatsumi, 2002; Leat and Larter, 2003; Smith et al., 2003a,b). These felsic magmas have been modelled as partial melts of the basaltic arc crust in what significantly represents a stage in the development of continental crust in an oceanic setting. This concept has important consequences for our understanding of the development and growth of continental crust which hitherto has generally been considered to be a process characteristic of continental arcs.

One of the reasons why the petrogenesis of intra-oceanic arcs is relatively poorly known is that samples are derived mainly from submarine dredge hauls where the stratigraphic relationships between samples can only be inferred and where comprehensive sampling is precluded. For example, recent submarine mapping of the Kermadec Arc (e.g. Wright et al., 1996; Wright and Gamble, 1999; Wright et al., 2002) has revealed a surprising abundance of siliceous rocks in dredge hauls and in many cases these are spatially associated with calderas resulting from relatively large siliceous eruptions (Smith et al., 2003b) but details of their stratigraphic relationships are unknown.

Three of the Kermadec Islands have subaerial exposures of siliceous rocks (Raoul, Macauley and Curtis; Smith et al., 2003b) but only on Raoul Island is there a sequence representing a series of felsic eruptions over an appreciable length of time. In this paper we present mineralogical and whole rock geochemical data for the young (<4 ka) siliceous rocks on Raoul Island. We argue that these represent independent products of an oceanic magmatic system that has evolved into a thermal stage where crustal reprocessing has produced felsic magmas.

2. Raoul Volcano

Raoul Island is the northernmost of the emergent volcanoes of the Kermadec Arc. It is a small island with maximum dimensions of 10 by 7 km and a total area of 29.4 km^2. It is the summit of a much larger volcanic massif with a volume of 214 km^3 and base dimensions of 28 by 20 km that rises 900 m from the crest of the Kermadec Ridge. The island is dominated by two adjacent collapse structures (Fig. 1). Raoul Caldera is approximately 3 by 2 km across and occupies the central part of the island; Denham Caldera forms the western margin of the island and is mostly submarine (Worthington et al., 1999).

Despite its small size, the volcanic deposits that make up the island record a complex history of eruptive events that reflect a variety of magmatic processes. The stratigraphy of the island has been described by Brothers and Searle (1970) and Lloyd and Nathan (1981). The stratigraphically lower units represent successive subaerial stratocone-building episodes constructed on a base of submarine volcanics and calcareous sediments which has an age of the order of 1 Ma (Lloyd and Nathan, 1981). The range in composition of the rocks forming these formations is basalt to basaltic andesite.

An abrupt change from mainly effusive cone-building eruptions of basalt and basaltic andesite lava to explosive eruptions dominated by pyroclastic deposits of dacitic composition occurred at 3.7 ka. There is no evidence for earlier dacitic magmatism although the preservation potential of older tephra on the island is low and little is known of the submarine portion of the volcano. Silicic magmatism began with the collapse of Raoul caldera during events known as the Matatirohia and Oneraki

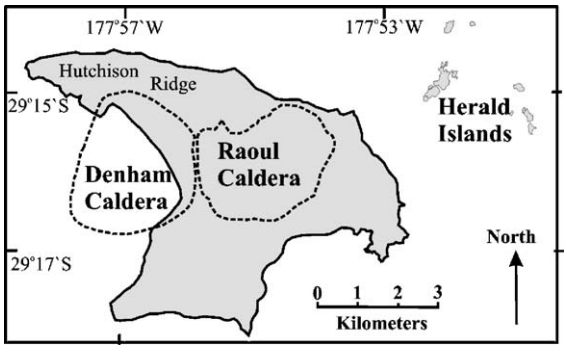

Fig. 1. Sketch map of Raoul Island and the adjacent Herald Islets showing the calderas (modified from Lloyd and Nathan, 1981).

eruptions, and culminated with the collapse of Denham Caldera during the voluminous Fleetwood eruption (Lloyd and Nathan, 1981). Subsequently there have been thirteen eruptions on a smaller scale at intervals of several hundred years or less. Five of these were silicic, two basaltic andesite and six phreatic (Lloyd and Nathan, 1981; Worthington et al., 1999). These events and their possible vent sources are listed in Table 1. The total volume of dacite magma erupted since 3.7 ka is approximately 15 km^3. The products of the eruptions are pumiceous fall and flow deposits and explosion breccia. These are exposed mainly along the north coast and cap Hutchison Ridge in the northwest of the island.

The Fleetwood Tephra (Lloyd and Nathan, 1981) is the largest of the young dacite eruptives and consists of 40 m of thick poorly-bedded pumice fall beds overlain by an 80 m thick cross-bedded pyroclastic flow and surge unit. The preferential orientation of carbonised logs in basal exposures is consistent with a Denham Caldera source. Worthington et al. (1999) estimate the volume of the eruption as >8 km^3. The Matatiro Tephra and Oneraki Tephra are also relatively large and consist of mainly poorly bedded Plinian pumice deposits up to 13 m thick. Because of their limited subaerial distribution their volume cannot be estimated but they represent eruptions that were smaller than that which produced the Fleetwood Tephra. The subsequent eruptions from Raoul Volcano were relatively smaller in volume and consist of bedded pumice fall deposits.

Table 1
Stratigraphy of the <3.7 ka eruption events from Raoul Volcano

Eruption	Age (ka)	Brief description of eruption and lithology	Source
1964		Phreatic; eruption breccia	Raoul Caldera
1870		Phreatic; eruption breccia	Raoul Caldera
Smith	0.18	Phreatic; eruption breccia	Raoul Caldera
Tui	.28	Phreatic; eruption breccia	Raoul Caldera
Sentinel	.28	Small; pumiceous dacite	Denham Caldera
Rangitahua	.37	Small; pumiceous dacite	Raoul Caldera
Meyer	0.5	Small; Scoraceous basaltic andesite	Meyer Islands
Expedition	1.10	Phreatic eruption breccia	Raoul Caldera
Pukekohu	1.25	Phreatic eruption breccia	Raoul Caldera
Green Lake	1.40	Medium; pumiceous dacite	Raoul Caldera
Rayner	1.55	Small; pumiceous dacite	Raoul Caldera
Judith	1.85	Medium; Scoraceous basaltic andesite	Denham Caldera
Bell	2.05	Small; pumiceous dacite	Denham Caldera
Fleetwood	2.20	Voluminous; pumiceous dacite, pyroclastic flows	Denham Caldera
Oneraki	3.15	Large; pumiceous dacite pyroclastic flows	Raoul Caldera
Matatirohia	3.70	Large; pumiceous dacite pyroclastic flows	Raoul Caldera

The ages of the eruptive events from Raoul Volcano are constrained by ^{14}C dating or interpolation between ^{14}C dates (Lloyd and Nathan, 1981).

3. Mineralogy of the dacites

Raoul Island dacites occur mainly as pumiceous breccia produced by pyroclastic eruptions. Most of the samples used in this study are pumice clasts although dense black obsidian samples have been collected from the Fleetwood, Oneraki and Matatirohia Formations. The pumice clasts vary in colour from dark to light grey to pink and typically contain <5% total phenocrysts. Obsidian clasts are dense, lack vesicles and are therefore considerably more phyric (3–10% total phenocrysts).

In general the pumice samples are strongly vesiculated (averaging 80% vesicles) although their total range in vesicularity is 10% to >90%. Vesicles range from 0.1 to >4.0 mm across and from strongly elongate to spherical (rarely polygonal). The groundmass consists of colourless glass except in pumice from Rangitahua Formation where it is pale brown and bears plagioclase microlites. Flow banding is common and is defined by the sub-parallel elongation of vesicles, layers with different vesicle sizes or degree of vesicularity, or the orientation of groundmass plagioclase.

Pumiceous clasts contain sparse subhedral to anhedral plagioclase phenocrysts <1.2 mm across; these often occur as subrounded clusters of 2–5 crystals sometimes including smaller crystals of pyroxene. The other main phenocryst phases are clinopyroxene and orthopyroxene and their modal abundance is less than that of plagioclase. Magnetite occurs as small phenocrysts and as inclusions in silicate phenocrysts. Plagioclase, the dominant crystal phase in nearly all Raoul lavas, ranges up to 45 vol.% in some of the mafic lavas. In dacite, plagioclase occurs as sparse crystals <5 vol.%.

The compositional range in the interior of crystals in both mafic and felsic rock types is remarkably similar, An_{50-96} in basalt/andesite and An_{50-98} in dacite. Compositional zoning within cores to near the crystal rims is oscillatory and the range of compositions within zones seldom exceeds 5 mol% An. Rim compositions are

normally zoned to more sodic compositions but also show a wide range $An_{60–88}$ in basalt/andesite and $An_{46–92}$ in dacite. The magnitude of the compositional change in any one crystal rim is typically 20–30 mol% An. These compositional variations are illustrated in Fig. 2.

Experimental studies of plagioclase–melt-equlibria have demonstrated a strong dependence of plagioclase composition on melt chemistry and H_2O content as well as temperature and pressure (Kudo and Weill, 1970; Baker and Eggler, 1987; Housh and Luhr, 1991; Sisson and Grove, 1993). From experiments on a synthetic, subduction-related basalt, Panjasawatwong et al. (1995) derived an empirical equation for the equilibrium near-liquidus plagioclase composition in an anhydrous melt. Using this equation the calculated An contents for Raoul Island dacite compositions are $An_{45–55}$ at 1200 °C and lower for temperatures between 900 and 1100 °C at pressures of 0.5 Gpa the lowest of the experiments. These results are shown in Fig. 3. Extrapolating to still lower pressures raises the calculated An content by about 10%. Plagioclase core compositions in basaltic and intermediate compositions are mostly more calcic but overlap calculated compositions for pressures of 0.5 Gpa and the overlap is greater at extrapolated lower pressures.

In summary, plagioclase interiors in both mafic and felsic rocks from Raoul Volcano are too calcic to be in equilibrium with their host magmas. Their weak zoning patterns indicate little variation in parent magma composition until an abrupt change to much more sodic compositions represented by their 10–25 μm wide rims and groundmass plagioclase. Furthermore, all plagioclase phenocryst compositions in the representative basalt–andesite and dacite lavas have very similar compositions. We interpret these observations to indicate that the 'phenocrysts' grew in magma whose composition was considerably different to that of their current hosts. Their zoning profiles do not reflect disequilibrium caused by a sudden drop in pressure and/or water content immediately prior to eruption but instead record an adjustment to equilibrium with a new and unrelated host magma (c.f. Ewart et al., 1973).

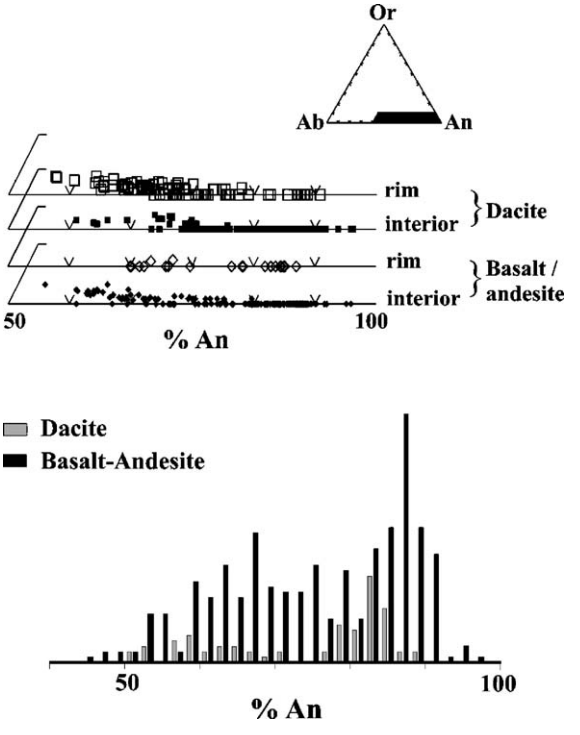

Fig. 2. Composition of plagioclase in representative mafic (basalt to andesite) and dacitic (>63 wt.% SiO_2) samples from Raoul Volcano.

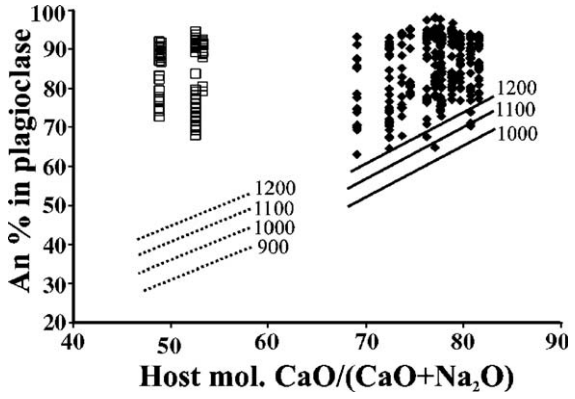

Fig. 3. Anorthite content of plagioclase in representative Raoul Volcano samples plotted against the theoretical liquidus plagioclase composition calculated from the whole rock composition using the formula of Panjasawatwong et al. (1995). Solid lines are the loci of liquidus plagioclase compositions calculated from basalt–andesite and the dotted lines are those for dacite.

The other main silicate phenocryst phase in Raoul siliceous rocks is pyroxene although modal abundance is less than that of plagioclase. Both clino- and orthopyroxene are present in the whole range of Raoul samples but orthopyroxene is relatively less common. As with plagioclase, clinopyroxene phenocrysts also exhibit minimal zoning except within 40 μm of their groundmass rims. The interior of these phenocrysts is commonly too iron-rich for equilibrium with their present host and they must also have crystallised from a magma with a different composition.

The compositions in representative samples are illustrated in Fig. 4. Core rim compositional relationships show the anticipated pattern of zoning toward more Fe-rich compositions at crystal rims. Clinopyroxene compositions in the dacites almost entirely overlap those in mafic samples. Dacite orthopyroxene compositions are slightly offset from those of basalt/andesite samples.

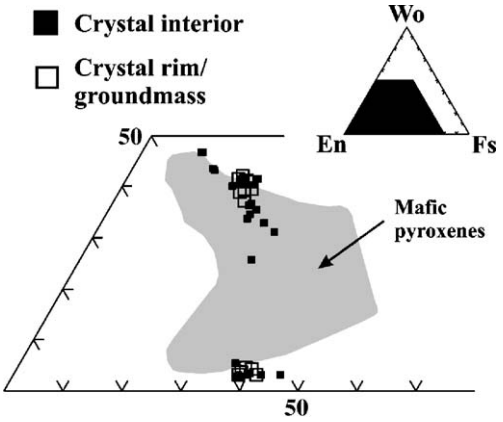

Fig. 4. Composition of pyroxene in Raoul dacite. The shaded area shows the compositional field of pyroxene in mafic rocks from Raoul Island.

When compared with calculated equilibrium compositions using host whole rock compositions (Fig. 5) most mafic sample pyroxenes are too iron-rich but both types of pyroxene in the dacites include compositions that could have crystallised from a magma with the whole rock composition. The majority of clinopyroxene phenocrysts in dacite also have interior and rim compositions that are too Fe rich for equilibrium with their host magma although they vary considerably in composition.

Interpretation of these data is equivocal. A case can be made for plagioclase crystals in both mafic and silicic rocks from Raoul that the interior of crystals did not

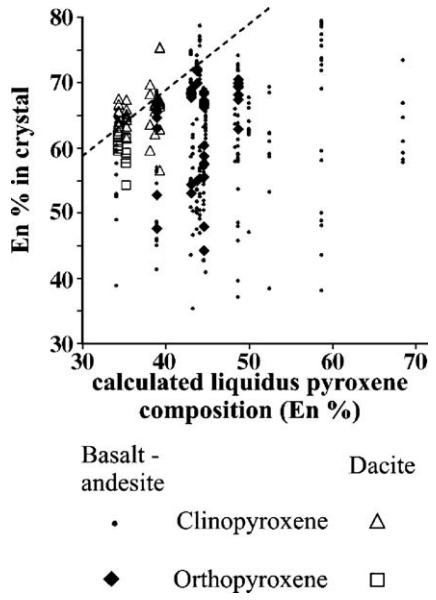

Fig. 5. Compositions of pyroxene in Raoul samples. Dashed line is locus of calculated pyroxene compositions in equilibrium with whole rock composition.

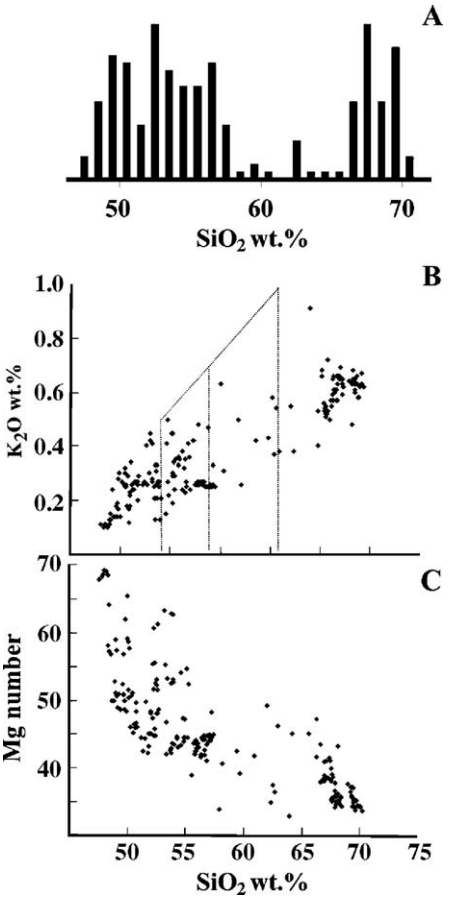

Fig. 6. Major element compositions of Raoul Island samples. A — histogram of SiO_2 (wt.%) content in 208 samples. B — Plot of SiO_2 (wt.%) against K_2O (wt.%). The fields and nomenclature are those of Gill (1981). C — Plot of Mg-number (mol% MgO/(MgO+FeO) against SiO_2 abundance.

crystallise from a liquid with the composition of the whole rock. The pyroxene data is less clearly interpreted but the coincidence of compositions in both mafic and felsic samples suggests that here also the crystals did not originate in a magma with the host rock composition.

A basic assumption in interpreting igneous rocks is that the crystals that they contain crystallised from a magma with the composition of the host rock. An assessment of phenocryst–melt equilibria in samples from Raoul volcano in general and particularly for the dacites suggests that this has not been the case.

4. Geochemistry

The predominant rock type on Raoul Island is porphyritic plagioclase-bearing relatively high-Al (typically >16 wt.% Al_2O_3) basalt–basaltic andesite although there is a range of compositions at any particular

Table 2
Chemical compositions of representative dacite samples from Raoul Island

AU number	23404	23394	46339	46334	23392	23398	46319	46315	46320	23401	46309
Unit	GL	M	R	R	R	F	GL	GL	GL	S	GL
(wt.%)											
SiO_2	65.09	65.34	65.66	66.07	66.63	67.08	67.71	67.80	68.47	68.89	69.49
TiO_2	0.59	0.50	0.66	0.65	0.66	0.48	0.59	0.58	0.59	0.60	0.59
Al_2O_3	14.03	15.07	14.69	14.72	14.58	13.39	13.98	13.93	14.32	13.95	14.08
Fe_2O_3	5.91	5.70	6.32	6.28	6.28	5.31	5.24	5.18	5.26	5.28	5.15
MnO	0.17	0.17	0.19	0.20	0.21	0.17	0.19	0.18	0.20	0.17	0.18
MgO	1.92	1.69	1.66	1.69	1.68	1.18	1.29	1.31	1.22	1.18	1.12
CaO	4.19	5.88	5.53	5.51	5.59	4.33	4.63	4.57	4.73	4.51	4.53
Na_2O	3.31	3.05	3.25	3.22	3.29	3.53	3.81	3.88	3.50	3.44	3.52
K_2O	0.63	0.54	0.50	0.52	0.50	0.64	0.62	0.62	0.59	0.62	0.61
P_2O_5	0.14	0.11	0.14	0.14	0.14	0.11	0.15	0.15	0.16	0.15	0.15
H_2Ond	1.02	0.19	0.06	0.07	0.10	0.25	0.11	0.15	0.07	0.20	0.04
LOI	2.77	1.52	0.95	0.75	0.14	3.26	1.30	1.57	0.49	1.11	0.29
Total	99.77	99.76	99.61	99.82	99.80	99.73	99.62	99.92	99.60	100.10	99.75
ppm											
Ba	227.1	185.4	197.5	185.2	195.7	197.1	209.0	194.6	203.6	207.7	212.0
Rb	9.5	8.0	7.4	7.4	7.9	10.2	8.6	7.9	9.1	8.9	8.7
Sr	150.4	160.3	173.3	171.4	174.0	152.9	166.3	165.1	167.2	166.2	169.7
Pb	7.7	4.1	5.2	5.0	6.9	4.9	3.2	3.6	3.3	4.6	3.5
Zr	77.0	67.9	71.9	72.0	73.0	76.9	79.1	78.9	80.7	80.4	80.0
Nb	1.9	1.7	1.8	1.7	1.6	1.8	1.8	1.9	1.8	1.8	1.8
Y	38.4	35.6	39.3	39.1	39.3	40.5	42.4	41.8	42.5	42.2	40.7
La	2.88	2.43	3.22	3.54	3.07	2.67	3.99	3.99	3.49	2.64	3.95
Ce	8.27	6.77	9.00	9.30	8.74	7.27	10.23	10.23	10.22	7.62	10.38
Nd	8.00	6.74	9.58	9.04	8.66	7.27	11.42	11.13	10.34	8.04	10.98
Sm	2.52	2.55	3.25	2.97	2.86	2.59	3.74	3.70	3.39	2.70	3.48
Eu	0.95	0.81	1.06	1.08	1.10	0.88	1.13	1.11	1.08	0.89	1.18
Gd	3.70	3.31	4.59	4.38	4.26	3.55	4.68	4.75	4.78	3.87	4.78
Dy	4.67	4.42	5.42	5.32	5.28	5.06	6.03	6.04	5.69	5.17	5.91
Er	2.80	nd	3.38	3.31	3.00	nd	3.73	3.77	3.58	n/a	3.78
Yb	2.95	2.89	3.49	3.42	3.11	3.24	3.82	3.77	3.68	3.41	3.83
Lu	0.49	0.46	0.56	0.54	0.52	0.55	0.60	0.59	0.59	0.54	0.62
Sc	24.3	21.5	23.6	24.5	27.0	17.4	22.4	21.9	20.3	23.3	24.3
V	70.9	65.5	60.5	62.7	62.5	41.9	25.6	27.5	27.0	27.9	22.6
Cr	11.3	10.9	6.8	5.8	5.3	5.3	5.1	5.4	6.3	4.6	5.2
Ni	5.8	5.1	2.5	2.2	3.2	1.2	3.3	3.1	2.1	2.4	2.0
Cu	26.6	30.9	8.2	9.6	7.2	12.2	8.2	8.9	5.5	7.4	5.0
Zn	103.7	82.4	105.6	112.5	106.9	91.4	96.9	93.9	91.8	95.3	82.9
Ga	15.3	15.3	16.1	16.2	16.1	14.7	14.5	14.6	15.0	15.7	15.0

Analyses by X-ray fluorescence except for the rare earth elements La to Lu which were analysed by ICP-OES.

SiO_2 content. A subordinate lava type is relatively high iron basalt–andesite (>12 wt.% FeO total), which is typically aphyric to sparsely porphyritic. Most of these rocks are geochemically evolved with low MgO contents (<6 wt.% MgO) and Mg-numbers [Mol% MgO/(MgO+FeO)] that are <55 (Fig. 6). The rocks that make up Raoul Island have sub-alkaline low-K compositions in terms of general concepts of arc-type associations. A histogram of 208 analysed samples from Raoul Island shows a clear bimodal distribution consisting of two sub-populations and very few lavas in the range 58–65 wt.% SiO_2; an observation previously made by Lloyd and Nathan (1981).

The post 3.7 ka dacite eruptions have a limited compositional range from 66–70 wt.% SiO_2 and in variation diagrams (Fig. 6.) plot along an extrapolation of the mafic lava array for most elements. The Mg-numbers of the dacites are relatively high (32–45) and partly overlap the range of more mafic compositions. These general features of the Raoul Island sequence were noted by Brothers and Searle (1970) and by Lloyd and Nathan (1981). For this study 52 dacite samples were analysed for major and trace element abundances by X-ray fluorescence and a representative sub-set analysed for rare earth element abundances by inductively coupled plasma optical emission spectroscopy (ICP-OES). Table 2

Table 3
Isotopic ratios in representative samples from Raoul Volcano

AU number	SiO_2	$^{87}Sr/^{86}Sr$	$^{143}Nd/^{144}Nd$	$^{206}Pb/^{204}Pb$	$^{207}Pb/^{204}Pb$	$^{208}Pb/^{204}Pb$
7135	47.85	0.70342	0.51306	18.648	15.571	38.342
7114	48.84	0.70349	0.51305	18.662	15.558	38.316
46357	49.01	0.70341	0.51303	18.685	15.577	38.371
7125	49.52	0.70340	0.51305	18.639	15.563	38.343
46329	51.44	0.70347	0.51304	18.652	15.566	38.333
46330	51.46	0.70345	0.51304	18.656	15.556	38.305
7144	51.48	0.70346	0.51305	18.656	15.565	38.316
46325	51.67	0.70353	0.51305	18.647	15.555	38.286
7148	51.78	0.70343	0.51305	18.659	15.571	38.387
7090	53.26	0.70345	0.51304	0.000	0.000	0.000
7053	54.83	0.70346	0.51304	18.643	15.546	38.268
7096	55.36	0.70347	0.51305	18.646	15.556	38.332
46362	55.53	0.70352	0.51307	18.667	15.574	38.356
46358	56.50	0.70349	0.51305	18.656	15.559	38.320
46368	56.77	0.70352	0.51305	18.641	15.565	38.319
7088	57.27	0.70353	0.51303	18.636	15.555	38.288
46339	65.66	0.70359	0.51307	18.649	15.550	38.311
46334	66.07	0.70358	0.51304	18.667	15.572	38.379
46290	66.28	0.70350	0.51305	18.672	15.569	38.356
46316	68.44	0.70354	0.51305	18.661	15.562	38.334
46320	68.47	0.70355	0.51305	18.662	15.565	38.342

presents representative analyses illustrating the range of compositions observed; the full data set is available from the authors.

Fresh pumice fragments were soaked in distilled water, rinsed and dried. These clean fragments were crushed between tungsten carbide plates and a 100 g aliquot of each sample ground to <200 mesh in a tungsten carbide ring grinder. Major element concentrations were determined by X-ray fluorescence using standard techniques using a Seimens SRS 3000 spectrometer. Trace element analyses used the same instrument calibrated using a suite of 36 international standards. Data reduction used Siemens SPECTRA 3000 software; the Compton scatter of X-ray tube line Rh $K\hat{a}_1$ was used to correct for mass attenuation and appropriate corrections were used for those elements analysed at energies below the Fe absorption edge. Precision is better than 1% for Sr and Zr, 1–3% for V, Cr, Zn and Y, 3–5% for Ba, 5–10% for Rb and Nb, 10–20% for Pb and more than 20% for La and Th. Detection limits are <2 ppm for Rb, Sr, Y, Zr. REE analyses were by ICP-OES. Approximately 2 g of rock powder was digested in several stages using a combination of acids in a sealed bomb. A REE concentrate was produced using cation exchange chromatography and the resulting solution analysed using an ARL 3410 spectrometer. A small number of representative samples were analysed for isotopic ratios (Table 3) using thermal ionisation mass spectrometry at La Trobe University, analytical techniques are detailed in Price et al. (1999).

The Fleetwood Formation (>8 km^3 of dacitic magma) is represented by 14 clasts that are a random collection through the lower fall deposits (~ 40 m thick on Hutchison Ridge); these include highly vesicular pumice, dense obsidian and lithic blocks. The chemical analyses of these samples are identical within analytical error except for one outlier (Fig. 7). The remainder of the analysed dacite data set consists of 8 samples from Rangitahua Formation, 16 from Green Lake Formation, 2 from Rayner formation, 5 from Oneraki Formation and 7 from Matatiro Formation. These samples are also a random selection through the stratigraphy of a each unit. Within analytical error all samples from Rangitahua, Green Lake, Rayner and Matatirohia Formations were identical to other samples from their respective tephra unit. From this observation each of these tephras is inferred to represent a homogeneous magma batch. Conversely 3 analyses from Oneraki Formation have disparate compositions.

Rare earth element (REE) abundances in the dacites show a small range that is positively correlated with SiO_2 content and the relative abundance patterns are essentially the same (Fig. 8). Chondrite normalised REE abundance patterns are light depleted with a small negative Eu anomaly. They lie at the top end of the REE abundance range shown by the mafic samples from Raoul.

Sr, Nd and Pb isotope ratios for a small number of representative samples are presented in Table 3 and their variation illustrated in Fig. 9. In terms of $^{87}/_{86}Sr$ ratios the Raoul Volcano dacites overlap the basalt/andesite range and extend to higher values. Nd isotope ratios and Pb isotope ratios for dacites overlap those of basalt/andesite. These variation patterns are similar to those observed for nearby Macauley Island by Smith et al. (2003a). The Raoul data lie on the regional Tonga and Kermadec trends definer by Hergt and Hawkesworth (1994), Gamble et al. (1996) and Turner et al. (1997).

5. Discussion

In subduction-related volcanic arcs emplaced in intra-oceanic settings or on young continental lithosphere, geochemical variation has generally been explained in terms of source variability and simple crystal fractionation models (e.g. Foden, 1983; Ewart and Hawkesworth, 1987). This is in marked contrast to models for the petrogenesis of subduction-related magmas that have evolved in mature continental settings. For continental arcs more complex models are generally invoked

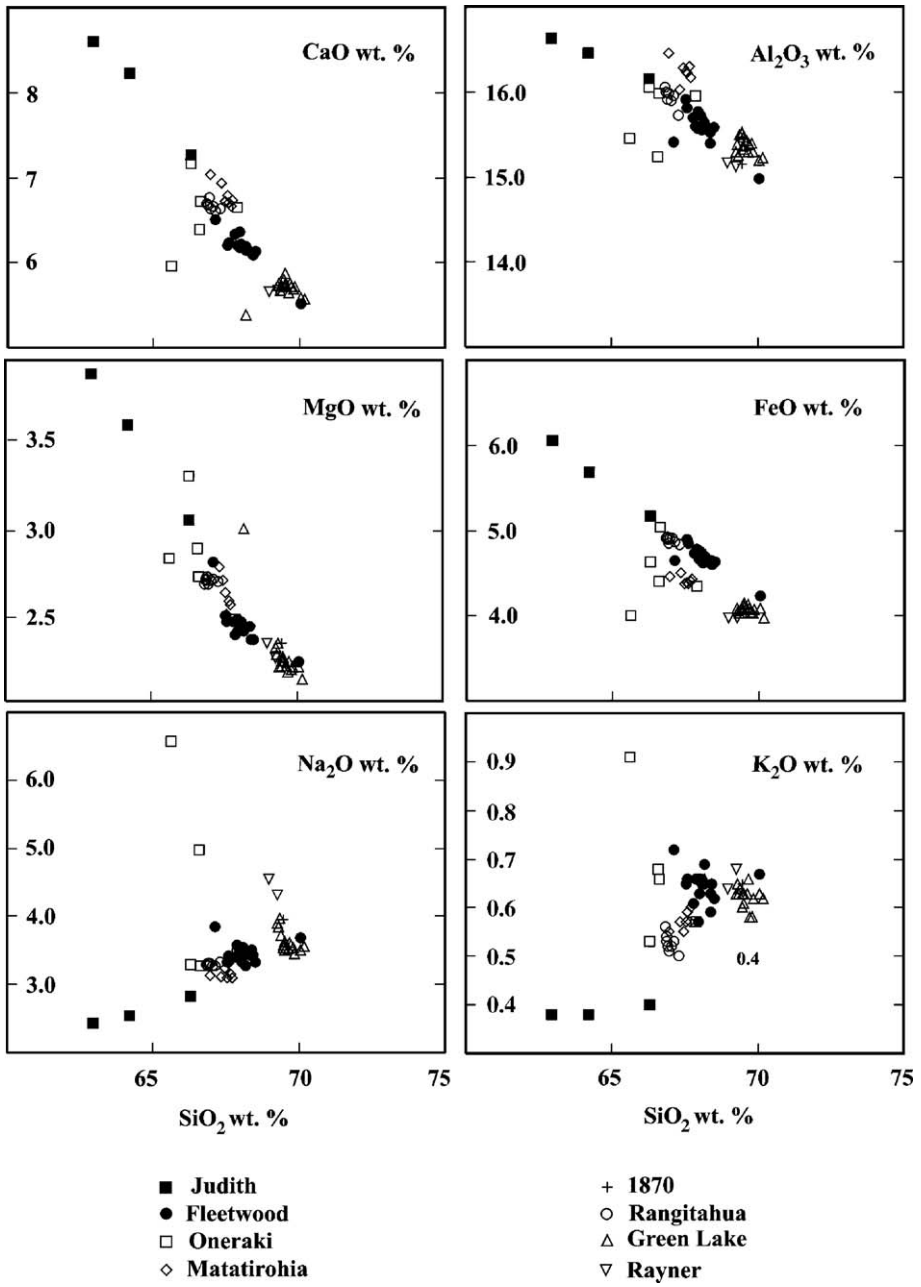

Fig. 7. Variation diagrams of selected major element oxides for Raoul dacites.

involving crustal assimilation, fractional crystallisation and magma mixing (e.g. McBirney, 1977; Eichelberger, 1978; Grove et al., 1982; Grove and Kinzler, 1986; Graham and Hackett, 1987; Feeley and Davidson, 1994; Dungan et al., 2001). In a number of studies of continental arcs, the role of crustal melting has been given prominence, particularly where rhyolitic magmas dominate (e.g. Ewart et al., 1975; Graham et al., 1992; Price et al., 2005) and there is a considerable body of literature concerned with thermal modelling of crustal melting. Several studies have demonstrated the feasibility of generating significant volumes of granitic/rhyolitic magma through either repeated intrusions of basalt (e.g. Huppert and Sparks, 1988; Petford and Gallagher, 2001; Annen and Sparks, 2002; Dufek and Bergantz, 2005) into sedimentary or amphibolitic crust or by underplating crust with basaltic magma (e.g. Bergantz, 1989; Laube and Springer, 1998).

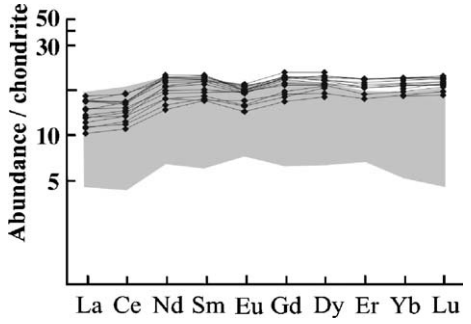

Fig. 8. Chondrite-normalised REE abundances of Raoul dacites. The shaded field is that of mafic samples from Raoul. Normalising values from Wasson and Kallemeyn (1988).

A recently published study by Berlo et al. (2004) used U-series isotopes to test partial melting hypotheses for the origin of Mt St Helens dacites and concluded from ^{226}Ra data that thermal incubation of crustal melts must be rapid or that even where crustal melting and/or assimilation are involved mantle derived basalts less than a few thousand years old must also be a significant component in the magmatic processes by which silicic magmas are produced in arcs.

The following discussion uses the data presented in this paper to evaluate simple crystal fractionation and crustal anatexis models for the origin of Raoul dacites.

5.1. Crystal fractionation as an origin for Raoul dacites

We have used the trends shown by the chemical compositions of the Raoul dacite suite erupted during the last 3.7 ka yr to assess whether the geochemical variation can be adequately modelled in terms of simple closed system fractional crystallisation. We have assumed that the phases that could contribute to the extract assemblage are plagioclase, clinopyroxene and magnetite which do occur as crystals in the modal assemblage of the dacites, and hornblende which is a potential phase in the mid-crustal environment beneath Raoul Island.

Evidence for a progressive change in the compositions of magma erupted from Raoul volcano through time is equivocal. There is an apparent increase in SiO_2 content from Matatirohia to Fleetwood, Reyner and Green Lake followed by an hiatus in volcanic activity and then a second cycle from Rangitahua to 1870 dacite. Alternatively magma vented from Denham Caldera could represent one cycle of increasing SiO_2 content with time from Fleetwood to 1870 dacite operating independently of a similar cycle at Raoul caldera from Matatirohia to Rayner and Green Lake followed by a second cycle beginning with Rangitahua (Fig. 10). However, other incompatible elements expected to show similar changes with fractionation processes (e.g. Zr, Ba) exhibit different and random variation with time (Fig. 11).

Significant compositional differences exist between each of the 5 homogeneous dacite magma batches (Rangitahua, Green Lake, Rayner, Fleetwood, Matatirohia) The single analysis of the 1870 dacite is also distinct from all the other dacites as are the 3 Oneraki analyses; a single analysis of Sentinel Formation is indistinguishable from Green lake Formation and is grouped with them in the diagrams. In general, compositional differences between these dacites are of sufficient magnitude that each forms a distinct field on variation diagrams (Fig. 7).

The dacites form well defined linear trends on variation diagrams (Figs. 7, 11, and 12). For example, there is a progressive decrease in V abundance with increasing wt.% SiO_2 through Matatirohia, Rangitahua, Fleetwood and Green Lake (Fig. 12). Fractional crystallisation exerts a powerful influence over both the V and SiO_2 contents and the linear V-SiO_2 trend thus imposes three constraints on models involving fractional crystallisation, namely, constant oxygen fugacity, a common

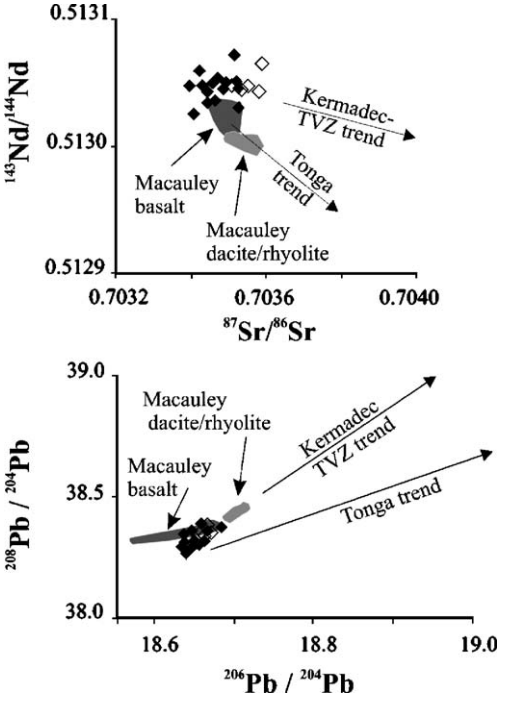

Fig. 9. Isotopic compositions for Raoul Island samples. Shaded fields represent Macauley Island basalts (dark) and dacites (light) from Smith et al. (2003a). The data defining regional Tonga and Kermadec trends are from Hergt and Hawkesworth (1994), Gamble et al. (1996) and Turner et al. (1997).

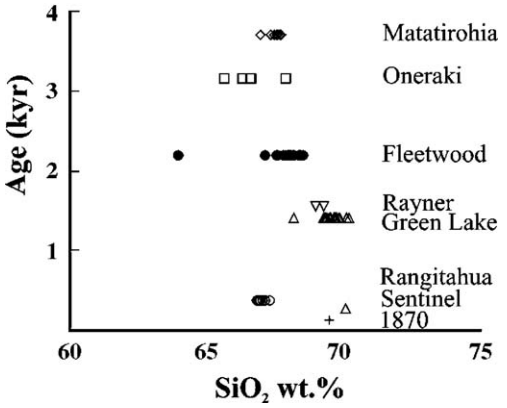

Fig. 10. SiO_2 variation with time through the dacite sequence on Raoul Island.

parent magma, and a constant extract assemblage. This process must also be self-repeating in order to connect Rangitahua, one of the youngest eruptions with Matatiroia, one of the oldest. Models proposing different parent magmas for each dacite require a fortuitous blend of starting compositions oxygen fugacity and extract assemblages to generate the linear trend.

There is a similarly well defined linear trend of decreasing TiO_2 abundance with increasing SiO_2 content through Rangitahua, Fleetwood, Rayner and Green Lake dacite. However, Matatirohia dacite plots off this trend and has markedly lower TiO_2 abundance at a given SiO_2 content. Matatiro dacite is the oldest in the sequence yet it cannot be parental to the younger tephra unless the extract assemblage consisted of sodic plagioclase and quartz and that combination does not work because Matatiro dacite has the lowest Na_2O content of any of the dacites (Fig. 7). If the dacites were derived from a common parent by fractional crystallisation then the mineral proportions in the extract assemblage must have been different when Matatirohia dacite was generated. Alternatively Matatirohia dacite was derived from a different parent magma.

Similar results are obtained from some other variation diagrams. Matatirohia Rangitahua Fleetwood Green Lake and 1870 dacite form a linear trend of increasing Ba abundance with increasing Zr content consistent with fractionation of plagioclase, hornblende and minor titaniferous magnetite from a common parent (Fig. 12). However, Rayner dacite plots off this trend and has lower Ba concentrations at similar Zr contents. It is inferred that either the extract assemblage from a common parent magma was different during the production of Rayner dacite, or that Rayner dacite has a different parental magma. Conversely Matatirohia dacite forms an integral part of the linear Ba–Zr trend.

The dacites have a scattered distribution on a plot of Zr concentration vs. SiO_2 abundance with each tephra except 1870 dacite forming a distinct field. The data distribution on this diagram (Fig. 11) is difficult to explain using fractional crystallisation models as no combination of plagioclase, hornblende, clinopyroxene or titaniferous magnetite can link the dacite batches in their eruption sequence. Instead quartz and plagioclase must fractionate to increase Zr abundance at constant SiO_2 concentration and produce the trend from Matatirohia to Fleetwood dacite yet Fleetwood dacite has a higher Na_2O content. To explain the lower Zr contents and higher SiO_2 abundances in the Rayner dacite, zircon must replace quartz in the extract assemblage but, at a later stage, quartz must again replace zircon so that Zr contents can increase at constant SiO_2 abundance and produce Green Lake dacite. A second cycle is required for Rangitahua dacite as it has far less Zr and SiO_2 relative to Green Lake dacite. Clearly most dacite batches cannot be directly related to each other. For fractional crystallisation models the importance of the observed Zr–SiO_2 variation is that either each dacite batch is derived from a common parent but features a different extract assemblage or, alternatively each dacite batch is derived from a different parent magma. Both of these possibilities stand in direct contradiction to the well

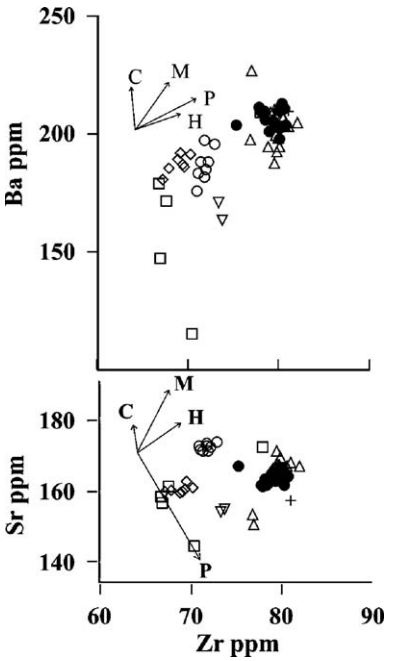

Fig. 11. Co-variation of Ba and Sr with Zr. Lines show trends described by fractional crystallisation by plagioclase (P), clinopyroxene (C) hornblende (H) titaniferous magnetite (M). Symbols as for Fig. 7.

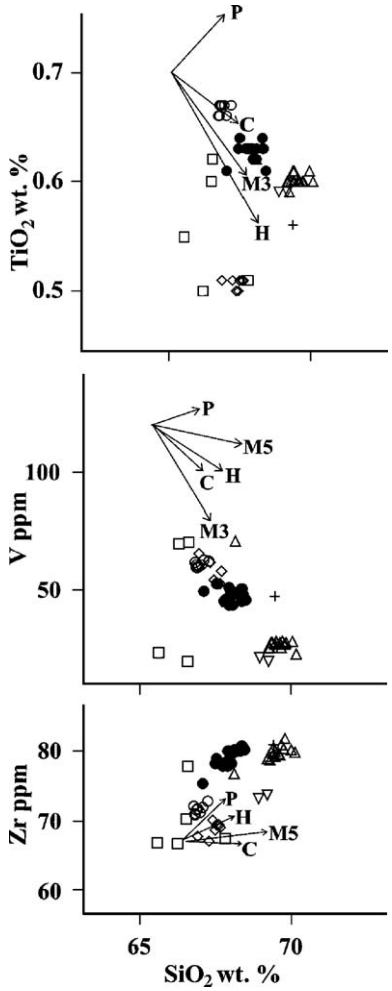

Fig. 12. Co-variation of TiO_2, V and Zr with SiO_2. Lines show trends described by 10% fractional crystallisation by plagioclase (P), clinopyroxene (C) hornblende (H) and 3% and 5% titaniferous magnetite (M3, M5) from a low-Si dacite composition. Symbols as for Fig. 7.

defined linear trends observed in variation diagrams (Figs 7, 10, and 11) for four or more tephra.

Plagioclase is expected to be the dominant phase in the extract assemblage of any fractional crystallisation model applicable to the dacites and the co-variation of Sr with Zr is sensitive to the proportion of plagioclase in the extract assemblage because Sr is compatible in plagioclase. Each dacite forms a distinct field on a plot of Sr content vs. Zr abundance (Fig. 11). Although some dacites can be linked in their eruption sequence (e.g. Matatirohia—Fleetwood, Rayner—Green Lake, Rangitahua—1870) the proportion of plagioclase relative to hornblende and titaniferous magnetite in the extract assemblage must differ in each instance. The same conclusion is reached if a common parent is assumed.

In summary most of the dacite tephras on Raoul represent homogeneous, geochemically distinct magma batches. Attempts to model the variations between these magma batches by fractional crystallisation lead to numerous contradictions. Well-defined linear trends on some variation diagrams provide strong evidence that the dacites were derived from a common parent magma by the removal of an extract assemblage of constant composition. Other element co-variation patterns demonstrate that the dacites cannot be derived from each other, cannot be derived from a common parent unless the composition of the extract assemblage varied for each magma batch, and are more consistent with a different parent for each dacite batch.

5.2. Crustal anatexis

Many features of the post 3.7 ka dacites on Raoul Island that are obstacles to petrogenetic models invoking fractional crystallisation do not present problems for models based on crustal anatexis. For example the sparsely phyric character of all post-3.7 ka dacites and their almost complete lack of groundmass crystals is suggestive of near-liquidus primary magmas unmodified prior to eruption. Competing fractionation models must find an efficient method of consistently removing phenocrysts of all sizes down to groundmass laths from the magma. The chemical evidence that at least some of the apparent phenocrysts in the dacites are xenocrystic also argues against a crystal fractionation model.

The offset in the value of Sr isotopic ratios observed in the Raoul dacites compared with more mafic rock types is consistent with an origin from crust that has had some time to evolve isotopically and more difficult to explain in a simple fractionation model. The similarity in the ratios of longer lived isotope pairs in both mafic and felsic rocks is consistent with either hypotheses and does not preclude an origin in relatively young arc crust.

Anatectic models have seldom been proposed for intra-oceanic felsic magmas perhaps because the sub-arc crust has been perceived as anhydrous gabbroic cumulates with high fusion temperatures. However, several recent publications (Tamura and Tatsumi, 2002; Leat et al., 2003; Smith et al., 2003b) argue strongly for crustal anatexis in oceanic arcs and this is supported by experimental work (Nakajima and Arima, 1998; Patino Douce, 2005).

The generation of dacitic magmas in an oceanic setting requires the existence of a fertile source and the means to exceed its solidus temperature. Under anhydrous conditions the temperatures required are

unlikely in any reasonable tectonic setting. However, the temperatures of the solidus under increasingly hydrous conditions are achievable even at the relatively modest pressures expected in the lower to middle crust of oceanic arcs. As Smith et al. (2003b) point out hydrous solidus temperatures may be achieved by the transfer of heat energy by the flux of magma through the crust provided that enough time is available. Estimates of the amount of time required to raise the lower crust to melting conditions given reasonable rates of magma flux converge on time scales of about 1 ma (Smith et al., 2003b).

Thermal models are consistent with a crustal melting origin for dacitic magmas in oceanic subduction settings. Laube and Springer (1998) developed numerical models for generating crustal melts through underplating at continental margins but they argued that their model is generally applicable to any arc setting. A similar approach was used by Annen and Sparks (2002) but they proposed that felsic melts could be generated by crustal melting associated with repeated intrusion of mafic magma rather than by underplating. They concluded that, over time intervals of the order of 10^5–10^6 years, multiple intrusion and crustal melting could produce areas within the crust of partially molten rock that could be periodically tapped to produce felsic eruptions. Felsic magmas were argued to contain two end-member components; re-melted basaltic lower crust and material derived by fractional crystallisation from the intruding and crystallising, mantle-derived magmas. Most recently, Dufek and Bergantz (2005) used a similar approach to model crustal melting arising from multiple dyke intrusion in a variety of settings. They used these models to suggest that distinct melting and mixing environments will develop in different arc settings according to crustal thickness, crustal age, and the mantle-derived magma flux. They concluded that where the crust is thin and mantle-derived magma fluxes relatively low, isolated pods of both mantle-derived and crustal melts will pond in the crust and will, in each case evolve and converge on dacite or rhyolite compositions.

Berlo et al. (2004) have evaluated the time-scales of these processes by modelling U-series disequlibria. They noted that significant levels of Ra excess observed in some dacites (e.g. Mt. St Helens) cannot be explained if such rocks are generated by simple melting of old crust and concluded that the Annen and Sparks (2002) models can only be reconciled with U-series isotopic data if a young, mantle-derived component is directly involved in the generation of felsic magmas. One possibility is that evolved felsic melts are mixed with young, less evolved material shortly before eruption. Alternatively inherited Ra excesses must indicate rapid crystallisation and short time scales for the extraction of evolved felsic melts from the lower crust.

Recent widespread felsic volcanism is a feature of the Tonga–Kermadec Arc despite its simple tectonic setting. Caldera forming eruptions at Raoul, Macauley and elsewhere along the arc may have been triggered by a transfer of extensional stress from the backarc Havre Trough to these volcanoes along en echelon rift grabens (Worthington et al., 1999). However, this does not explain the origin of dacitic magma. A consistent explanation emerges from the record of magmatism exposed on Raoul Island. The earlier part of the exposed succession consists only of mafic rocks reflecting the long term flux of subduction-related magmatism. In the last 3.7 ka this pattern has been disrupted by an influx of siliceous magmas. One scenario that arises from our observations of Raoul is that the evolution of the magmatic system has reached an ‘adolescent’ stage in which a fertile source has reached a point in which dehydration of amphibole has fluxed the source and promoted melting. One consequence of this is the creation of an infertile residue that is no longer able to generate melts. If this is the case then Raoul is passing through an adolescent window of siliceous magmatism and will return in the future to a mature stage of mafic magmatism.

The record of siliceous volcanism from Raoul Volcano provides evidence of multiple eruption of different dacitic compositions at frequent intervals. It suggests that the mafic and felsic components of the magmatic system are closely coupled spatially. It shows that magmas in oceanic systems are open systems and that the concept of large magma chambers hosting volumes of silicic magma that has developed in continental settings is open to question.

This model has parallels in the continental setting. For example Price et al. (2005) propose that in the Taupo Volcanic Zone at the southern end of the Tonga–Kermadec system, andesitic magmatism shows increasing crustal involvement with time and suggest that andesitic magmatism may eventually evolve into siliceous magmatism.

Acknowledgements

We would like to acknowledge the New Zealand Lottery Grants Board who supported field work on Raoul Island (Lottery Science Grant SR022590) and John Young of the yacht Blackadder who provided unrivalled logistic support in the Kermadec Islands. We also acknowledge the University of Auckland Research Committee for providing grants to support analytical

work at University of Auckland and support provided by La Trobe University and the Australian Research Council.

References

Annen, C., Sparks, R.S.J., 2002. Effects of repetitive emplacement of basaltic intrusions on thermal evolution and melt generation in the crust. Earth Planet. Sci. Lett. 203, 937–955.

Baker, D.R., Eggler, D.H., 1987. Compositions of anhydrous and hydrous melts coexisting with plagioclase, augite and olivine or low-Ca pyroxene from 1 atm to 8 kbar: application to the Aleutian volcanic centre of Atka. Am. Mineral. 72, 12–28.

Beard, J.S., 1995. Experimental, geological and geochemical constraints on the origins of low-K silicic magmas in oceanic arcs. J. Geophys. Res. 100, 15593–15600.

Bergantz, G.W., 1989. Underplating and partial melting: implications for melt generation and extraction. Science 245, 1093–1095.

Berlo, K., Turner, S., Blundy, J., Hawkesworth, C.J., 2004. The extent of U-series disequilibria produced during partial melting of the lower crust with implications for the formation of the Mount St. Helens dacites. Contrib. Mineral. Petrol. 148, 122–130.

Bloomer, S.H., Stern, R.J., Smoot, N.C., 1989. Physical volcanology of the submarine Mariana and volcano arcs. Bull. Volcanol. 51, 210–224.

Brothers, R.N., Searle, E.J., 1970. The geology of Raoul Island, Kermadec Group, southwest Pacific. Bull. Volcanol. 34, 7–37.

Crawford, A.J., Greene, H.J., Exon, N.F., 1988. Geology, petrology and geochemistry of submarine volcanoes around Epi Island, New Hebrides island arc. In: Greene, H.G., Wong, F.L. (Eds.), Geology and Offshore resources of Pacific Island Arcs-Vanuatu Regions. Circum-Pacific Council Energy Min. Res., Houston Texas, pp. 301–327.

Dufek, J., Bergantz, G.W., 2005. Lower crustal magma genesis and preservation: a stochastic framework for the evaluation of basalt–crust interaction. J. Petrol. 46, 2167–2195.

Dungan, M.A., Wulff, A., Thompson, R., 2001. Eruptive stratigraphy of the Tatara–San Pedro Complex, 36°S, southern volcanic zone, Chilean Andes: reconstruction method and implications for magma evolution at long-lived arc volcanic centers. J. Petrol. 42, 555–626.

Eichelberger, J.C., 1978. Andesitic volcanism and crustal evolution. Nature 275, 21–27.

Ewart, A., Hawkesworth, C.J., 1987. The Pleistocene – Recent Tonga–Kermadec arc lavas: interpretation of new isotopic and rare earth data in terms of a depleted mantle source model. J. Petrol. 28, 495–530.

Ewart, A., Bryan, W.B., Gill, J.B., 1973. Mineralogy and geochemistry of the younger volcanic islands of Tonga, S.W. Pacific. J. Petrol. 14, 429–465.

Ewart, A., Hildreth, W., Carmichael, I.S.E., 1975. Quaternary acid magma in New Zealand. Contrib. Mineral. Petrol. 51, 1–27.

Feeley, T.C., Davidson, J.P., 1994. Petrology of calc-alkaline lavas at Volcán Ollagüe and the origin of compositional diversity at central Andean stratovolcanoes. J. Petrol. 35, 1295–1340.

Fiske, R.S., Naka, J., Iizasa, K., Yuasa, M., Klaus, A., 2001. Submarine silicic caldera at the front of the Izu–Bonin arc, Japan: voluminous seafloor eruptions of rhyolite pumice. Geol. Soc. Amer. Bull. 113, 813–824.

Foden, J.D., 1983. The petrology of the calcalkaline lavas of Rindjani Volcano, East Sunda Arc: a model for island arc petrogenesis. J. Petrol. 24, 98–130.

Gamble, J.A., Woodhead, J.D., Wright, I.C., Smith, I.E.M., 1996. Basalt and sediment geochemistry and magma petrogenesis in a transect from oceanic island arc to rifted continental margin arc: the Kermadec–Hikurangi margin southwest Pacific. J. Petrol. 37, 1523–1546.

Gill, J.B., 1981. Orogenic Andesites and Plate Tectonics. Springer-Verlag, New York. 390 pp.

Gill, J.B., Seales, C., Thompson, P., Hochstaedter, A.G., Dunlap, C., 1992. Petrology and geochemistry of Pliocene–Pleistocene volcanic rocks from the Izu arc, Leg 126. In: Taylor, B., Fujioka, K., et al. (Eds.), Proceedings of the Ocean Drilling Program, Scientific Results, vol. 126. Ocean Drilling Program, College Station, TX, pp. 383–404.

Graham, I.J., Hackett, W.R., 1987. Petrology of calc-alkaline lavas from Ruapehu volcano and related vents, Taupo Volcanic Zone, New Zealand. J. Petrol. 28, 531–567.

Graham, I.J., Gulson, B.L., Hedenquist, J.W., Mizon, K., 1992. Petrogenesis of late Cenozoic volcanic rocks from the Taupo Volcanic Zone, New Zealand, in the light of new Pb isotope data. Geochim. Cosmochim. Acta 56, 2797–2819.

Grove, T.L., Kinzler, R.J., 1986. Petrogenesis of andesites. Annu. Rev. Earth Planet. Sci. 14, 417–454.

Grove, R.L., Gerlach, D.C., Sando, T.W., 1982. Origin of calc-alkaline series at Medicine Lake volcano by fractionation, assimilation and mixing. Contrib. Mineral. Petrol. 80, 160–182.

Hergt, J.M, Hawkesworth, C.J., 1994. Pb–Sr- and Nd-isotopic evolution of the Lau Basin: implications for mantle dynamics during backarc opening. In: Hawkins, J.W., Parson, L.M., Allan, J.F., et al. (Eds.), Proc. Ocean Drilling Program, Scientific Results, vol. 135. Ocean Drilling Program, College Station, Texas, pp. 505–517.

Housh, T.B., Luhr, J.F., 1991. Plagioclase–melt equilibria in hydrous systems. Am. Mineral. 76, 477–492.

Huppert, H.E., Sparks, R.S.J., 1988. The generation of granitic magmas by intrusion of basalt into continental crust. J. Petrol. 29, 599–624.

Kudo, A.M., Weill, D.F., 1970. An igneous plagioclase thermometer. Contrib. Mineral. Petrol. 25, 52–65.

Laube, N., Springer, J., 1998. Crustal melting by ponding of mafic magmas: a numerical model. J. Volcanol. Geotherm. Res. 81, 19–35.

Leat, P.T., Larter, R.D., 2003. Intra-oceanic subduction systems: introduction. In: Larter, R.D., Leat, P.T. (Eds.), Intra-Oceanic Subduction Systems: Tectonic and Magmatic Processes. Spec. Publ. Geol. Soc. Lond., vol. 219, pp. 1–18.

Leat, P.T., Smellie, J.L., Millar, I.L., Larter, R.D., 2003. Magmatism in the South Sandwich arc. In: Larter, R.D., Leat, P.T. (Eds.), Intra-Oceanic Subduction Systems: Tectonic and Magmatic Processes. Spec. Publ. Geol. Soc. Lond., vol. 219, pp. 285–313.

Lloyd, E.F., Nathan, S., 1981. Geology and tephrochronology of Raoul Island, Kermadec Group, New Zealand. N. Z. Geol. Surv. Bull., vol. 95. Government Printer Wellington. 105 pp.

McBirney, A.R., 1977. Mixing and unmixing of magmas. J. Volcanol. Geotherm. Res. 7, 357–371.

Miller, T.P., 1995. Late Quaternary caldera formation along the Aleutian arc: distribution, age and volume (abstract). EOS. Trans. Am. Geophys. Union., vol. 76, p. 680.

Monzier, M., Robin, C., Eisses, J.-P., 1994. Kuwae (~ 1425 A.D.): the forgotten caldera. J. Volcanol. Geotherm. Res. 59, 207–218.

Nakajima, K., Arima, M., 1998. Melting experiments on hydrous low-K tholeiite: implications for the genesis of tonalitic crust in the Izu–Bonin–Mariana arc. Isl. Arc 7, 359–373.

Panjasawatwong, Y., Danyushevsky, L.V., Crawford, A.J., Harris, K.L., 1995. An experimental study of the effects of melt composition on plagioclase–melt equilibria at 5 and 10 kbar: implications for the origin of magmatic high-An plagioclase. Contrib. Mineral. Petrol. 118, 420–432.

Patino Douce, A.E., 2005. Vapor-absent melting of tonalite at 15–32 kbar. J. Petrol. 46, 275–290.

Pearce, J.A., Baker, P.E., Harvey, P.K., Luff, I.W., 1995. Geochemical evidence for subduction fluxes, mantle melting and fractional crystallisation beneath the South Sandwich island arc. J. Petrol. 36, 1073–1109.

Petford, N., Gallagher, K., 2001. Partial melting of mafic (amphibolitic) lower crust by periodic influx of basaltic magma. Earth Planet. Sci. Lett. 193, 483–499.

Price, R.C., Stewart, R.B., Woodhead, J.D., Smith, I.E.M., 1999. Petrogenesis of high-K arc magmas: evidence from Egmont volcano, North Island, New Zealand. J. Petrol. 40, 167–197.

Price, R.C., Gamble, J.A., Smith, I.E.M., Stewart, R.B., Eggins, S., Wright, I.C., 2005. An integrated model for the temporal evolution of andesites and rhyolites and crustal development in New Zealand's North Island. J. Volcanol. Geotherm. Res. 140, 1–24.

Robin, C., Eissen, J.-P., Monzier, M., 1993. Giant tuff cone and 12 km-wide associated caldera at Ambryn volcano (Vanuatu, New Hebrides Arc). J. Volcanol. Geoth. Res. 55, 225–238.

Sisson, T.W., Grove, T.L., 1993. Experimental investigations of the role of H_2O in calc-alkaline differentiation and subduction zone magmatism. Contrib. Mineral. Petrol. 113, 143–166.

Smith, I.E.M., Stewart, R.B., Price, R.C., 2003a. The petrology of a large intra-oceanic silicic eruption: the Sandy Bay Tephra, Kermadec arc, Southwest Pacific. J. Volcanol. Geotherm. Res. 124, 173–194.

Smith, I.E.M., Worthington, T.J., Stewart, R.B., Price, R.C., Gamble, J.A., 2003b. Felsic volcanism in the Kermadec arc, southwest Pacific: crustal recycling in an oceanic setting. In: Larter, R.D., Leat, P.T. (Eds.), Intra-Oceanic Subduction Systems: Tectonic and Magmatic Processes. Special Publication of the Geological Society of London, vol. 219, pp. 99–118.

Tamura, Y., Tatsumi, Y., 2002. Remelting of an andesitic crust as a possible origin of rhyolitic magma in oceanic arcs: an example from Izu–Bonin arc. J. Petrol. 43, 1029–1047.

Turner, S., Hawkesworth, C., Rogers, N., Bartlett, J., Worthington, T., Hergt, J., Pearce, J., Smith, I.E.M., 1997. ^{238}U–^{230}Th disequilibria, magma petrogenesis and flux rates along the depleted Tonga–Kermadec island arc. Geochim. Cosmochim. Acta 61, 4855–4884.

Wasson, K., Kallemeyn, G.W., 1988. Compositions of chondrites. Philos. Trans. R. Soc. Lond. Ser. A: Math. Phys. Sci. 325, 535–544.

Worthington, T.J., Gregory, M.R., Bondarenko, V., 1999. The Denham Caldera on Raoul volcano: dacitic volcanism in the Tonga–Kermadec arc. J. Volcanol. Geotherm. Res. 90, 29–48.

Wright, I.C., Gamble, J.A., 1999. Southern Kermadec submarine caldera arc volcanoes (SW Pacific): caldera formation by effusive and pyroclastic eruption. Mar. Geol. 161, 207–227.

Wright, I.C., Parson, L.M., Gamble, J.A., 1996. Evolution and interaction of migrating cross-arc volcanism and backarc rifting: an example from the southern Havre Trough (35°20′–37°S). J. Geophys. Res. 101, 22071–22086.

Wright, I.C., Stoffers, P., Hannington, M., de Ronde, C.E.J., Herzig, P., Smith, I.E.M., Browne, P.R.L., 2002. Towed-camera investigations of shallow–intermediate water-depth submarine basaltic, strata volcanoes of the southern Kermadec arc. Mar. Geol. 185, 207–218.